Acoust. Sci. & Tech. **29**, 3 (2008)

PAPER

Coupling between two membranes of a Japanese drum

Hideo Suzuki[1] and Yun-Fan Hwang[2]

[1]*Department of Information and Network Science, Chiba Institute of Technology, 2–17–1 Tsudanuma, Narashino, 275–0016 Japan*
[2]*Feng-Chia University, 100 Wenhwa Road, Seatwen, Taichung, Taiwan, 40724, R. O. C.*

(*Received 12 October 2007, Accepted for publication 1 February 2008*)

Abstract: Some drums have, typically, a hollow trunk (or a barrel) with a circular membrane at each of the two ends. In this type of drum structure, the two membranes interact with each other through the air between them inside the body. Even if the two membranes have an identical fundamental resonance frequency, the interaction results in two resonance frequencies. At the lower resonance, the two membranes vibrate in phase. Since the membranes must move the internal air, the frequency at the lower resonance is lower than that of the original resonance (without air loading). At the higher resonance, they vibrate out-of-phase, causing compression or expansion of the internal air simultaneously. The frequency at this resonance is higher than that of the original resonance since, in this case, the air works as a spring. In this paper, resonance frequencies and mode shapes of the coupled membranes are investigated using an analytical model. The membranes are assumed to be ideal (i.e., no bending stiffness) and the body is assumed to be ideally rigid. Since it is a common practice that the two membranes are slightly (intentionally) miss-tuned, the main interest of this paper is to simulate the effect of this miss-tuning on the resulting resonance frequencies and mode shapes. Numerical results for the case of a 48 cm diameter and 50 cm length Japanese drum are presented.

Keywords: Drum, Membrane, Diaphragm, Coupling

PACS number: 43.75.Hi, 43.40.Dx [doi:10.1250/ast.29.215]

1. INTRODUCTION

The traditional Japanese drums are called "Wa-daiko." "Wa" means Japan and "d(t)aiko" means a (big) drum. A Chodo-daiko (the long body drum), with a membrane on each of the two ends of a barrel-like body (as shown in Fig. 1), is the most popular one in the Wadaiko family. Due to the fact that the chodo-daiko has such a simple structure, there are very few design parameters for manufacturers to control. Once the design of the drum is fixed, manufacturer-controlled variables include the selection of skins and the setting of tensions. It is a common practice for manufactures to use thinner skins and to stretch them with a higher tension for the rear membrane as opposed to the front membrane. One membrane is tuned while the other is almost in a fixed condition. Since the two membranes are strongly coupled, the resultant frequencies deviate from those at the time of tuning. Furthermore, the skins are made wet so that they can be stretched easily and tuned to a desired pitch while still wet. The resonance frequencies, however, will go up as the skins dry, and they will reach stable values after a couple of days. These are all done by experience and on a try-and-error basis. Therefore, the quantitative information obtained from a rigorous analysis may be helpful to improve the manufacturing process.

Few experimental studies have been reported on Japanese drums [1,2]. This paper theoretically investigates the coupling between the two membranes through the air inside the barrel, concentrating on the resonance frequency changes due to the coupling. The sound pressure inside the barrel is expressed by a series expansion of spherical Bessel and Legendre functions with unknown coefficients [3]. The displacement of the membrane, on the other hand, is expressed by a series expansion of cylindrical Bessel functions with unknown coefficients. Applying the least square error method on the continuity of the velocity and the equilibrium of force acting on the membranes, the eigen-frequencies and the corresponding modal shapes are obtained. The effects by the miss-tuning of the two membranes on the coupled resonance frequencies are then analyzed.

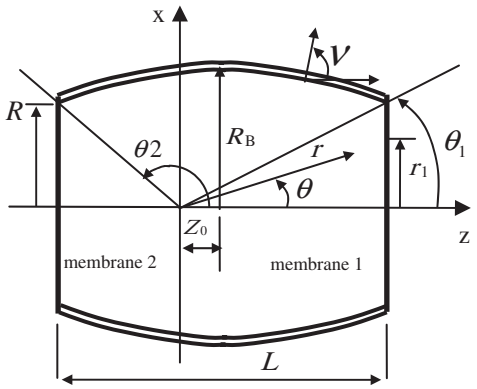

Fig. 1 Geometry of the model drum.

2. GEOMETRY AND MATERIAL PROPERTIES OF THE MODEL DRUM

The geometry of a Japanese model drum is shown in Fig. 1. The two membranes are attached at both ends of the barrel-like body (which will be called "barrel" hereafter). The drum is rotationally symmetric with respect to the z-axis. The origin of the coordinate system is off-set by Z_0 from the center of the drum. The drum is also symmetric with respect to the x-axis if $Z_0 = 0$. The ideally rigid barrel has the dimensions R (radius of the opening), R_B (maximum radius of the barrel) and L (total length) as shown in Fig. 1. The meridional curvature of the barrel is determined by a circle of radius, $R_c = (R_B - R)/2 + L^2/[8(R_B - R)]$, which passes through the mid point (located at (Z_0, R_B)) and the two edge points (located at $(Z_0 + L/2, R)$ and $(Z_0 - L/2, R)$) of the drum. The thicknesses, tensions and densities per unit area of membrane 1 and membrane 2 are h_1 and h_2, T_1 and T_2, and ρ_1 and ρ_2, respectively.

The location of an arbitrary point inside the drum is expressed by the polar coordinates (r, θ). The cylindrical coordinate ϕ is omitted because of the rotational symmetry. The regions $0 \le \theta \le \theta_1$, $\theta_1 \le \theta \le \theta_2$ and $\theta_2 \le \theta \le \pi$ represent the membrane 1, barrel, and membrane 2, respectively. A position on the membranes is also expressed using radius r_1. The outward vector normal to the membranes has the angle ν (equal to 0 and π for membrane 1 and 2, respectively).

3. MATHEMATICAL EXPRESSIONS OF THE MEMBRANE VIBRATION AND THE SOUND FIELD

3.1. Pressure Inside the Drum

It is known that, in the closed space without a source, the pressure in an axis-symmetric steady-state sound field at angular frequency ω can be expressed by [3,4]

$$p(r, \theta) = \sum_{n=0}^{\infty} a_n j_n(kr) P_n(\cos\theta) \tag{1}$$

where a_n is an unknown coefficient of the n-th order spherical Bessel (j_n) and Legendre (P_n) functions, and k ($= \omega/c$, c is the sound speed) is the wavenumber. The unknown coefficients will be determined from the boundary conditions.

3.2. Vibration of the Membrane

The steady-state free vibration of a membrane with tension T (N/m) and the density per unit area ρ (kg/m^2) is given by

$$(T\nabla^2 + \rho\omega^2) Y(r_1) = 0 \tag{2}$$

where ∇^2 is the Laplacian operator and $Y(r_1)$ is the displacement of the membrane at radius r_1. The solutions of Eq. (2) for a circular membrane are as follows:

$$Y(r_1) = J_n(\kappa r_1)\cos(n\phi) \tag{3}$$

where J_n is the cylindrical Bessel function of the n-th order and κ is the wavenumber of the membrane ($= \omega/\sqrt{T/\rho}$). It should be noted that the Neumann functions are omitted because they are singular at the origin. Furthermore, if only the axisymmetric modes are taken into consideration, the solution becomes

$$Y(r_1) = J_0(\kappa r_1) \tag{4}$$

The boundary condition

$$Y(R) = J_0(\kappa R) = 0 \tag{5}$$

gives the eigenvalues and the corresponding eigenfunctions. Eigenvalues are the values of $\kappa_m R$ ($m = 0, 1, 2, \ldots$) that satisfy

$$J_0(\kappa_m R) = 0 \tag{6}$$

and, the corresponding eigenfunctions are

$$Y_m(r_1) = J_0(\kappa_m r_1) \tag{7}$$

A solution of a forced vibration can be expressed by the summation of these functions with unknown coefficients, b_m, i.e.,

$$y(r_1) = \sum_{m=0}^{\infty} b_m J_0(\kappa_m r_1) \tag{8}$$

3.3. Equilibrium of Forces Acting on the Membranes

The equilibrium of the forces acting on the membranes for a steady-state vibration at angular frequency ω is expressed by

$$(T_i\nabla^2 + \rho_i\omega^2) y_i(r_1) = \mp p(r, \theta) \tag{9}$$

where the subscript i (1 or 2) indicates the quantities related to membrane 1 or 2, respectively. The minus and plus signs on the right-hand side correspond to $i = 1$ and 2, respectively. Substituting Eqs. (1) and (8) into Eq. (9) and using the relationship

$$\kappa_i^2 = \omega^2/(T_i/\rho_i) \tag{10}$$

we can rewrite Eq. (9) as

$$\sum_{m=0}^{M} b_m^i[-(\kappa_m)^2 + \kappa_i^2)]J_0(\kappa_m r_1) = \mp\frac{1}{T_i}\sum_{n=0}^{N} a_n j_n(kr)P_n(\cos\theta) \tag{11}$$

where b_m^i, $i = 1$ and 2, represent unknown coefficients for membrane 1 and 2, respectively. Numerical accuracy of the computation depends on the truncations of m and n, or the summation up to M and N, respectively. Using the orthogonal property of the Bessel functions [5]

$$\int_0^R J_0(\kappa_m r_1)J_0(\kappa_l r_1)2\pi r_1 dr_1 = \pi R^2[J_1(\kappa_m R)]^2 \tag{12}$$

the relations between b_m^i and a_n are obtained as follows:

$$b_m^i = \sum_{n=0}^{N}\left(\mp\frac{1}{T_i}\left[\int_{Si} j_n(kr)P_n(\cos\theta)J_0(\kappa_m r_1)ds\right] \Big/ [\{-(\kappa_m)^2 + \kappa_i^2\}\cdot S_i \cdot \{J_1(\kappa_m R)\}^2]\right)a_n = \sum_{n=0}^{N} A_{mn}^i a_n \tag{13}$$

where S_i is the area of the membrane i (1 or 2) and ds is the incremental area given by $ds = 2\pi r_1 dr_1$. It is noted that the expression for the term A_{mn}^i is shown explicitly in Eq. (13).

3.4. Continuity of the Velocities on the Internal Surface of the Drum

The sound pressure inside the drum is solely determined by the velocities normal to the interior surface of the drum. The velocities on the membranes are given by multiplying Eq. (8) by $j\omega$, and the velocity on the surface of the barrel is zero. For the continuity of the velocity, the membranes and the barrel velocities must be equal to the particle velocities normal to the internal drum surface.

The particle velocity inside the drum in the direction of angle ν is obtained from Eq. (1) as follows [4]:

$$\begin{aligned} v_\nu(r,\theta) &= -\frac{1}{j\omega\rho}\frac{\partial p(r,\theta)}{\partial \nu} \\ &= -\frac{1}{j\omega\rho}\sum_{n=0}^{N} a_n[k\cos\theta j_n'(kr)P_n(\cos\theta)\cos(\nu-\theta) \\ &\quad - j_n(kr)P_n'(\cos\theta)\sin(\theta)\sin(\nu-\theta)/r] \end{aligned} \tag{14}$$

On the surface S_1, the angle ν is 0, and the continuity condition is expressed by

$$v(r,\theta) = \sum_{n=0}^{N}\Psi_n^{(1)}a_n = \sum_{m=0}^{M}[j\omega J_0(\kappa_m r_1)]b_m^1 \tag{15}$$

where

$$\begin{aligned} \Psi_n^{(1)} &= \frac{1}{j\omega\rho}[-k\cos\theta j_n'(kr)P_n(\cos\theta)\cos(\theta) \\ &\quad - j_n(kr)P_n'(\cos\theta)\sin^2(\theta)/r] \end{aligned} \tag{16}$$

Using Eq. (13), Eq. (15) can be rewritten as

$$\sum_{n=0}^{N}\left[\Psi_n^{(1)}(r,\theta) - \sum_{m=0}^{M} j\omega J_0(\kappa_m r_1)A_{mn}^1\right]a_n = \sum_{n=0}^{N}\Phi_n^{(1)}a_n = 0 \tag{17}$$

Similarly, on the surface S_2 ($\nu = \pi$), we have

$$\sum_{n=0}^{N}\left[\Psi_n^{(2)}(r,\theta) - \sum_{m=0}^{M} j\omega J_0(\kappa_m r_1)A_{mn}^2\right]a_n = \sum_{n=0}^{N}\Phi_n^{(2)}a_n = 0 \tag{18}$$

where

$$\begin{aligned} \Psi_n^{(2)} &= \frac{1}{j\omega\rho}[-k\cos\theta j_n'(kr)P_n(\cos\theta)\cos(\theta) \\ &\quad + j_n(kr)P_n'(\cos\theta)\sin^2(\theta)/r] \end{aligned} \tag{19}$$

On the internal surface of the barrel, S_3, the particle velocity must satisfy

$$\sum_{n=0}^{N}\Psi_n^{(3)}a_n = \sum_{n=0}^{N}\Phi_n^{(3)}a_n = 0 \tag{20}$$

where

$$\begin{aligned} \Psi_n^{(3)} &= \frac{1}{j\omega\rho}[-k\cos\theta j_n'(kr)P_n(\cos\theta)\cos(\nu-\theta) \\ &\quad - j_n(kr)P_n'(\cos\theta)\sin(\theta)\sin(\nu-\theta)/r] \end{aligned} \tag{21}$$

The angle ν at point (r,θ) is determined from the geometry of the barrel shown in Fig. 1.

3.5. Least Square Error Method

All variables of $\Phi_n^{(1)}$, $\Phi_n^{(2)}$ and $\Phi_n^{(3)}$ are predetermined except the angular frequency ω. In order for the unknown coefficients a_n that satisfy Eqs. (17), (18), and (20) to be non-trivial, ω must take some specific values, which are the eigen-frequencies of the system. It is noted that these three equations are valid at any arbitrary point (r,θ) or r_1 in their respective regions. Since there are an infinite number of points to be satisfied and there will be implicitly an infinite number of linear equations for $N+1$ unknown coefficients. Therefore, we have an over-determined problem. For such a problem, the least-square-error method [3,4] may be applied for finding the solution.

When the error function is defined as

$$E = \int_{S_1} \left| \sum_{n=0}^{N} \Phi_n^{(1)} a_n \right|^2 ds + \int_{S_2} \left| \sum_{n=0}^{N} \Phi_n^{(2)} a_n \right|^2 ds + \int_{S_3} \left| \sum_{n=0}^{N} \Phi_n^{(3)} a_n \right|^2 ds \quad (22)$$

the least-square-error method gives $[N+1]$ simultaneous equations:

$$\sum_{n=0}^{N} p_{in} a_n = 0 \quad (i = 0, 1, 2, \ldots, N) \quad (23)$$

where

$$p_{in} = \int_{S_1} \Phi_i^{(1)*} \Phi_n^{(1)} ds + \int_{S_2} \Phi_i^{(2)*} \Phi_n^{(2)} ds + \int_{S_3} \Phi_i^{(3)*} \Phi_n^{(3)} ds \quad (24)$$

For a non-trivial solution of a_n, the determinant of the matrix $[P]$ with elements p_{in} must be zero. This makes it possible to find eigen-frequencies of the system. Once the eigen-frequencies are determined, the corresponding eigenvectors which are relative magnitudes of the coefficients a_n (and also b_m^1 and b_m^2), can be determined. It should be noted that $\Phi_n^{(i)}$ $(i = 1, 2, 3)$ are purely imaginary (and therefore p_{in} are purely real) if the loss of the system is not taken into account.

4. NUMERICAL EVALUATION OF THE COUPLING EFFECT

4.1. Geometry and Material Properties of the Model Drum

The following drum dimensions (internal) are employed: $R = 0.2\,\mathrm{m}$, $R_B = 0.24\,\mathrm{m}$, $L = 0.5\,\mathrm{m}$. Since the external shape of the barrel is circular, we assume that the internal shape is also circular. This enables us to calculate the radius of the circle (that determines the curvature of the barrel) from R, R_B, and L. Because of the reasoning that will be presented later, the origin of the coordinate system is offset by Z_0 $(= L/2.5)$ from the centre of the drum as shown in Fig. 1.

From the measurement of material properties of real cow skins, it is known that the volume density (d) and thickness (h) are roughly equal to $2{,}000\,\mathrm{kg/m^3}$ and 1.5–2 mm, respectively. There might be small reductions from these values due to the tension after the skin is stretched. However, we will use those values without modification. Since a real drum with the similar dimensions mentioned above has the lowest resonance frequency around (120 ± 20) Hz, we assume that the tension T of membrane 1 is equal to $14{,}000\,\mathrm{N/m}$, which gives a resonance frequency of 113.3 Hz. The properties of membrane 2 will be given first the same as, and later different from those of membrane 1. We assume $1.21\,\mathrm{kg/m^3}$ for the air density and 343 m/s for the speed of sound in the air. The cow skin, when ready for use as a diaphragm, has the Young's modulus of approximately $3.5 \times 10^9\,\mathrm{Pa}$. However, the effect of bending stiffness will be neglected in this analysis.

After several trials in the accuracy evaluation, the order of truncation of the series expansions, M and N, were set equal to 10 and 19, respectively.

4.2. Results for the Case with Identical Membranes

The eigen-frequencies can be obtained by finding the roots of the determinant D. The well known Newton-Raphson method has been frequently used for searching these roots. In the following discussion, an alternative root finding method which does not require an initial guess of the root and can be illustrated graphically, will be used.

A frequency dependence of the logarithm of the determinant D of the matrix $[P]$, $Det(f) = \log_{10} |D_P|$, for the case with identical properties of the two membranes $(T_1 = T_2 = 14{,}000\,\mathrm{N/m})$ is shown by the thick line in Fig. 2. As the curve shows, it has a very strong frequency dependency, and variations to display local minima of the function are not clearly seen. The thin line in Fig. 2 shows the result after the constant and linear components (as the result of regression) are removed from the original curve. In this modified curve, two minima at 110.5 and 120.0 Hz are now clearly seen (these two frequencies will be referred to as f_1 and f_2, respectively). The large peak at 113.3 (referred to as f_0) is due to the resonance without air loading. The separation between f_1 and f_2 is 0.12 octaves.

As mentioned in the previous section, once a specific frequency that minimizes the determinant of $[P]$ is found, the vector $\{a\}$ and then vectors $\{b^1\}$ and $\{b^2\}$ (Eq. (13)) at this frequency are determined if the assumption $a_1 = 1$ is employed. The displacements of the membrane 1 and 2 at the frequencies 110.5 Hz and 120.0 Hz are shown by the left and right charts in Fig. 3, respectively. The displacements of two membranes are almost the same in magnitude for both frequencies. With respect to the phase relationship, they are in the push-pull (in-phase) mode at 110.5 Hz and in the push-push (or pull-pull) mode at 120.0 Hz (out-of-phase). The two membranes behave equally since the drum is symmetric and membranes have identical properties. The

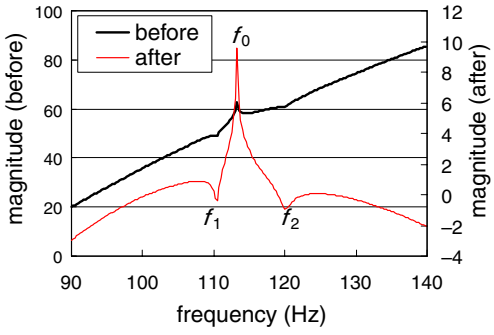

Fig. 2 Frequency dependence of the determinant of the matrix $[P]$.

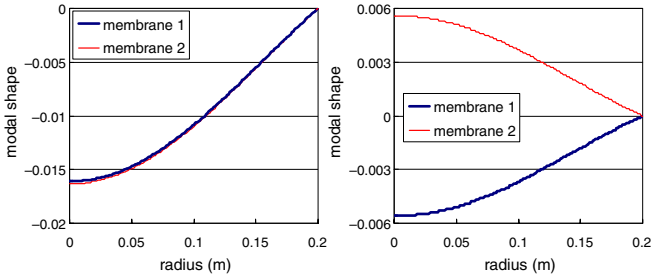

Fig. 3 Membrane displacements at f_1 (left) and f_2 (right).

frequency of the push-pull mode is lower than the load-free resonance because of the air mass loading. On the other hand, the push-push mode has a higher resonance frequency since the air is compressed severely, i.e., acting as a spring.

The displacements of the two membranes in the above figure do not match perfectly. This is caused by the offsetting of the origin by Z_0. If this offset is removed, the differences are negligible. In this case, however, we can get only the push-push mode. This is because the contributions by the odd order terms of a_n are removed due to the symmetry of the system. If only the odd order terms are used, we can have only push-pull mode. This is why the offsetting in the calculation is employed with a small sacrifice of accuracy.

The boundary conditions (continuity of the velocity) must be checked in order to evaluate the accuracy of the results. The thick and thin lines in Fig. 4 show magnitudes of velocities $|\Psi_n^{(i)}|$ $(i = 1, 2, 3)$ (Eqs. (16), (19), and (21)) and velocity differences (errors) $|\Phi_n^{(i)}|$ $(i = 1, 2, 3)$ (Eqs. (17), (18), and (20)) as functions of positions along the inner surface. Position number 1 to 200 correspond to the positions from the centre to the edge of the membrane 1, 201 to 400 along the barrel from right to left, and 401 to 600 from the edge to the centre of the membrane 2. The left and right side vertical axes show the values for $\Psi_n^{(i)}$ and $\Phi_n^{(i)}$, respectively. The errors of the velocity at the centres of the membranes are approximately 2.1% indicating that the boundary conditions are well satisfied. Two relatively large but narrow error peaks are observed at the junctions between the barrel and the diaphragms. This is still 4.5% of the maximum diaphragm velocity. The sign of the errors changes alternatively between plus and minus and therefore the total contribution may be smaller than it looks. The thick line shows that the particle velocity on the surface of the barrel is close to zero, or much smaller as compared to the membrane velocities.

The authors are also studying the same topic using the finite element method [6]. The vibration of the body, as well as the stiffness of the membranes, is taken into account in this model. The two lowest resonance frequencies obtained from the finite element method for the case with $T_1 = T_2 = 14{,}000\,\mathrm{N/m}$, a very small Young's modulus ($1 \times 10^6\,\mathrm{Pa}$) for the skin, and a large Young's modulus ($7.2 \times 10^{10}\,\mathrm{Pa}$) for the body, are 110.6 Hz and 119.5 Hz which are very close to those obtained in the present paper. The agreement of the resonance frequencies obtained by the two completely different methods may be a good indication of the validity of the present paper.

4.3. Results for the Cases with Different Properties of the Two Membranes

The frequency characteristics of the determinants for different tensions of membrane 2 are shown in Fig. 5 (a: 14,000 N/m, b: 15,000 N/m, c: 16,000 N/m, d: 17,000 N/m, e: 18,000 N/m, and f: 20,000 N/m). We can also see two minima for the unequal membranes. Curves "d" to "f" have higher f_1 than f_0. However, even if the tension is increased to 21,000 N/m, f_1 does not increase further from that for $T_2 = 20{,}000\,\mathrm{N/m}$. This is because the displacement of membrane 2 becomes smaller; thus membrane 2 functions almost like a rigid end plate, which does not interact with membrane 1. On the other hand, f_2 gets higher as the load-free resonance (f_0') of membrane 2 is increased.

Figure 6 shows the dependences of frequency ratios (f_1/f_0, f_2/f_0, and f_2/f_1) on the tension ratio (T_2/T_1). If $T_2 = T_1$, f_2 is 8.6% (0.12 octave) higher than f_1. If $T_2/T_1 = 1.2$, f_2 is approximately whole tone higher than

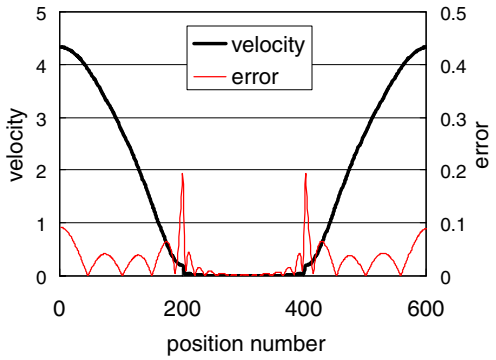

Fig. 4 Velocity (thick lines) and velocity errors (thin lines) along the inner peripheral of the model drum.

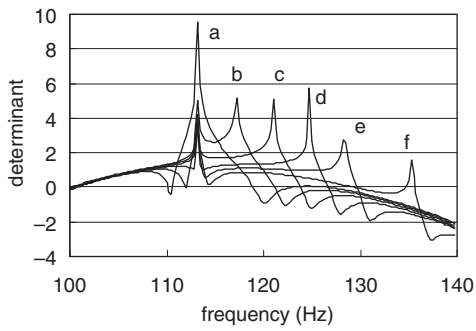

Fig. 5 Frequency dependence of determinants for various T_2 (a:14000, b:15000, c:16000, d:17000, e:18000, f:20000). T_1 is fixed at 14,000.

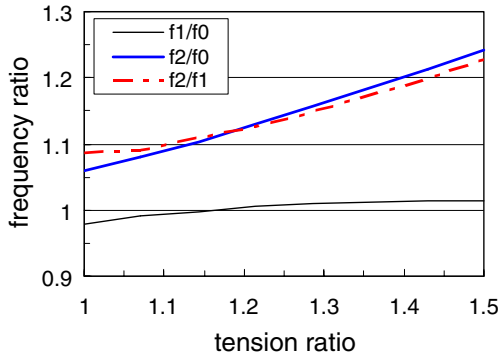

Fig. 6 Dependence of frequency ratios on the tension ratio.

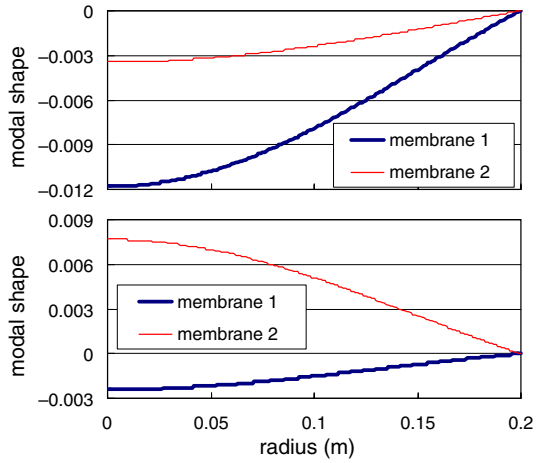

Fig. 7 Membrane displacements at f_1 (top) and f_2 (bottom) for the case of "e" in Fig. 5.

f_1. It is known from the figure that the frequency ratio (f_2/f_1) increases almost linearly as the (T_2/T_1) ratio is increased to over $T_2/T_1 = 1.35$. It is also known from the figure that f_1 becomes larger than f_0 when $T_2/T_1 \geq 1.15$.

The membrane displacements at f_1 and f_2 for curve "e" of Fig. 5 are shown in Fig. 7. As it is expected, the displacement of membrane 2 is smaller than that of membrane 1 at f_1. Their roles are then reversed at f_2.

4.4. Effect of the Lossfactor

The physical model that has been treated thus far is a system without loss. The easiest way to introduce a loss is to add modal damping to the membranes. This can be done by replacing $[-(\kappa_m R)^2 + \kappa^2]$ with $[-(\kappa_m R)^2 + \kappa^2 - j\eta\kappa(\kappa_m R)]$ in Eq. (11), where η is the loss factor. Figure 8 compares the determinant characteristics "e" for the case without loss and with a loss factor of 0.01. The effect of the loss factor to the determinant is similar to resonances and anti-resonances of a dynamic system.

5. CONCLUSIONS

The coupling of membranes through the air inside a Japanese drum body was analyzed using an analytical model. Only axisymmetric modes were considered and the coupling through the external air was neglected. The first lowest resonance is the push-pull (in-phase) mode, and the second lowest is the push-push (out-of-phase) mode. Depending on the tension ratio of the membranes, the frequency and amplitude ratios of the coupled resonances change. If the two membranes are tuned to be equal, the resonance frequencies are separated by 8.6% for the case analyzed here (48 cm diameter and 50 cm long chodo-daiko). If one membrane is tuned with a higher tension, the frequency separation increases.

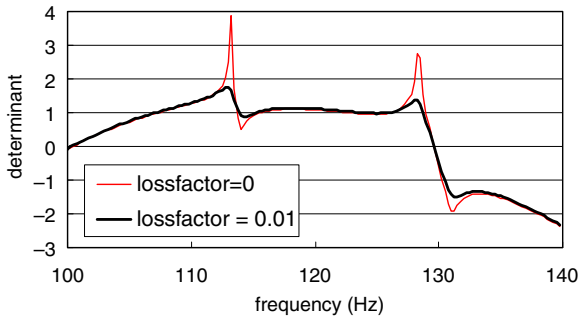

Fig. 8 Effect of the lossfactor on the determinant characteristics.

The method used here is a semi-analytic method and it may provide useful comparison (for accuracy and correctness) with results obtained from the other methods such as FEM and BEM methods. The modelling of Japanese drums including the vibration of the body and the couplings of internal and external air is under way. It is expected that the numerical results such as the resonance frequency spacing and modal behaviours for both axisymmetric and non-axisymmetric modes will be helpful in evaluating tone quality of Japanese drums.

ACKNOWLEDGEMENT

The authors would like to thank Miyamoto Unosuke Shouten Co., Ltd., for the many useful discussion on the tuning of Japanese drums.

REFERENCES

[1] T. D. Rossing, *Science of Percussion Instruments* (World Scientific, Singapore, 2000).
[2] J. Obata and T. Tesima, "Experimental studies on the sound and vibrations of drum," *J. Acoust. Soc. Am.*, **6**, 267–274 (1935).
[3] E. Skudryzyk, *The Foundations of Acoustics* (Springer-Verlag, Wien, 1971), p. 400.
[4] H. Suzuki and J. Tichy, "Sound radiation from convex and concave domes in an infinite baffle," *J. Acoust. Soc. Am.*, **69**, 41–49 (1981).
[5] S. Gradshteyn and I. M. Ryzhik, *Table of Integrals Series and Products* (Academic Press, New York, 1965), p. 672.
[6] Y. Hwang and H. Suzuki, "Numerical simulations of fluid-structure interactions in a Japanese drum," *ICA 2007*, SAV-02-002-IP (2007).